

Appendix to “Entrainment and motion of coarse particles in a shallow water stream down a steep slope”

By C. Ancey, A. Davison, T. Böhm, M. Jodeau and P. Frey

Journal of Fluid Mechanics, vol. 595 (2008), pp. 83–114

This material has not been copy-edited or typeset by Cambridge University Press: its format is entirely the responsibility of the author.

Supplementary figures

Figure 1 provides a snapshot of all experiments whose data were used for this paper. Figures 2 and 3 show the probability density function of N for experiments (a)–(o). The dots represent the empirical probabilities, while the dashed line stands for the negative binomial distribution (2.15), the parameters of which were estimated using the measured values $\text{Var}N$ and \bar{N} reported in Tables 1 and 2 in the main paper; for the sake of readability, we plotted the discrete probability mass functions as continuous curves.

Figures 4 and 5 show the autocorrelation functions of the total solid discharge, the number of moving beads, and the theoretical curve (2.21), where the autocorrelation time t_c is replaced by its estimate \hat{t}_c given by equation (2.22).

From time series such as that in Figure 5(a) in the paper, we can compute the lag times $\Delta t_{b \rightarrow m}$ between two deposition events within the observation window. We can then infer the statistical properties of the lag times $\Delta t_{b \rightarrow m}$. Figures 6 and 7 report the empirical probability distribution of $\Delta t_{b \rightarrow m}$ for runs (a)–(o). On the same figures, we have plotted the theoretical curve given by equation (2.27), which is an exponential density with parameter $t_\sigma^{-1} = (1-p)r\sigma/p = \bar{N}\sigma$.

If we plot the probability of observing $n_{m \rightarrow b}$ particles settling during a time interval $\delta t = 1/130$ s, there are less substantial differences between the theoretical and empirical distributions. Figures 8 and 9 show these probability distributions for runs (a)–(o). Theoretically, the number of settling particles follows the probability distribution (2.28) derived in § 2.6.

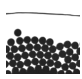
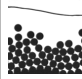
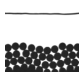
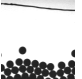
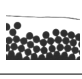
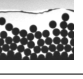
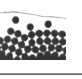
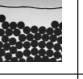
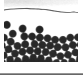
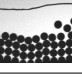
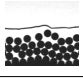
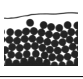
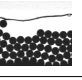
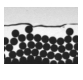
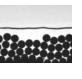
\dot{n} (beads/s) $\tan \theta$ (%)	6	7	8	9	11	16	21
7.5							
10							
12.5							
15							

Figure 1: Overview of the experiments conducted at various solid discharges \dot{n} and slopes $\tan \theta$. For each experiment, a detail of one filmed image is shown. See Tables 1 and 2 in the main paper for the experimental conditions.

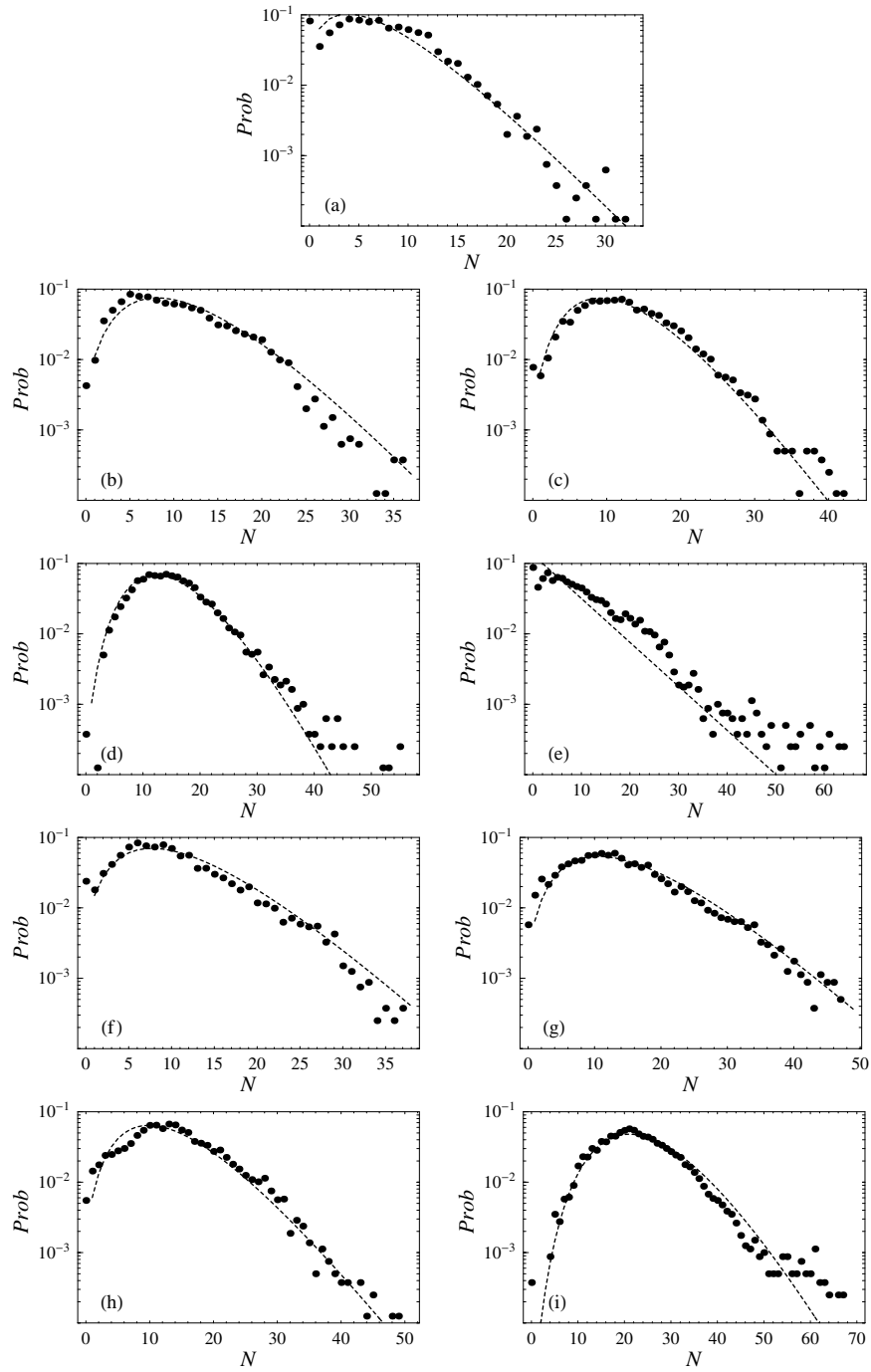


Figure 2: Empirical probability density of the total number of moving beads N (black dots). The dashed line is the probability density function of the negative binomial distribution. Experiments (a–i).

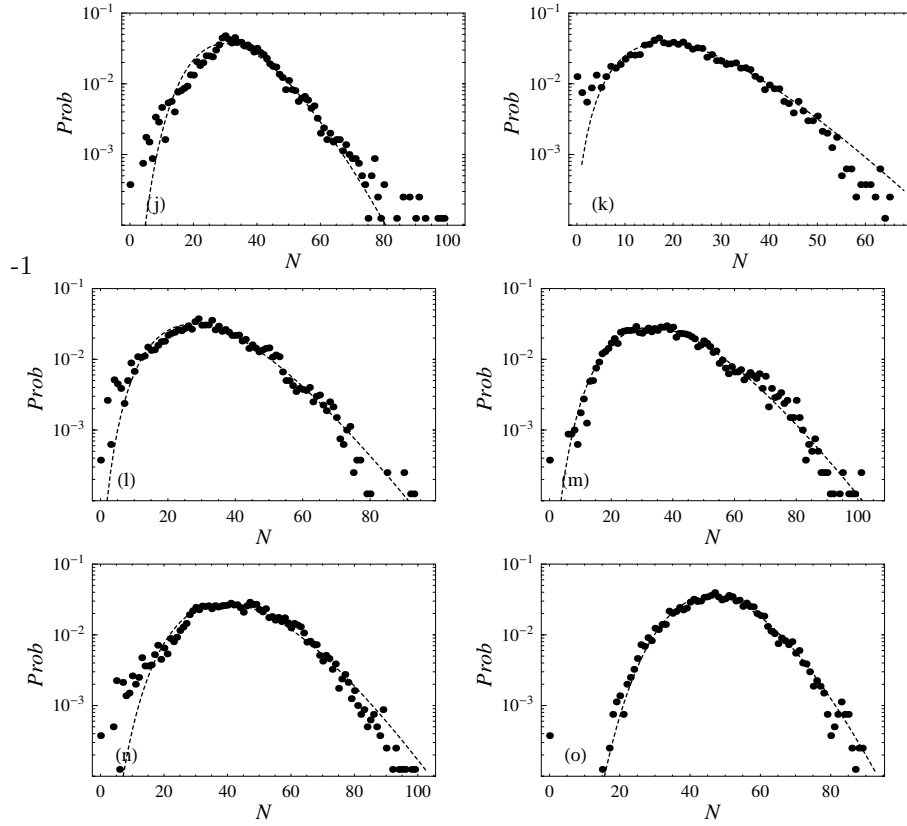


Figure 3: Continuation of figure 2, for experiments (j–o).

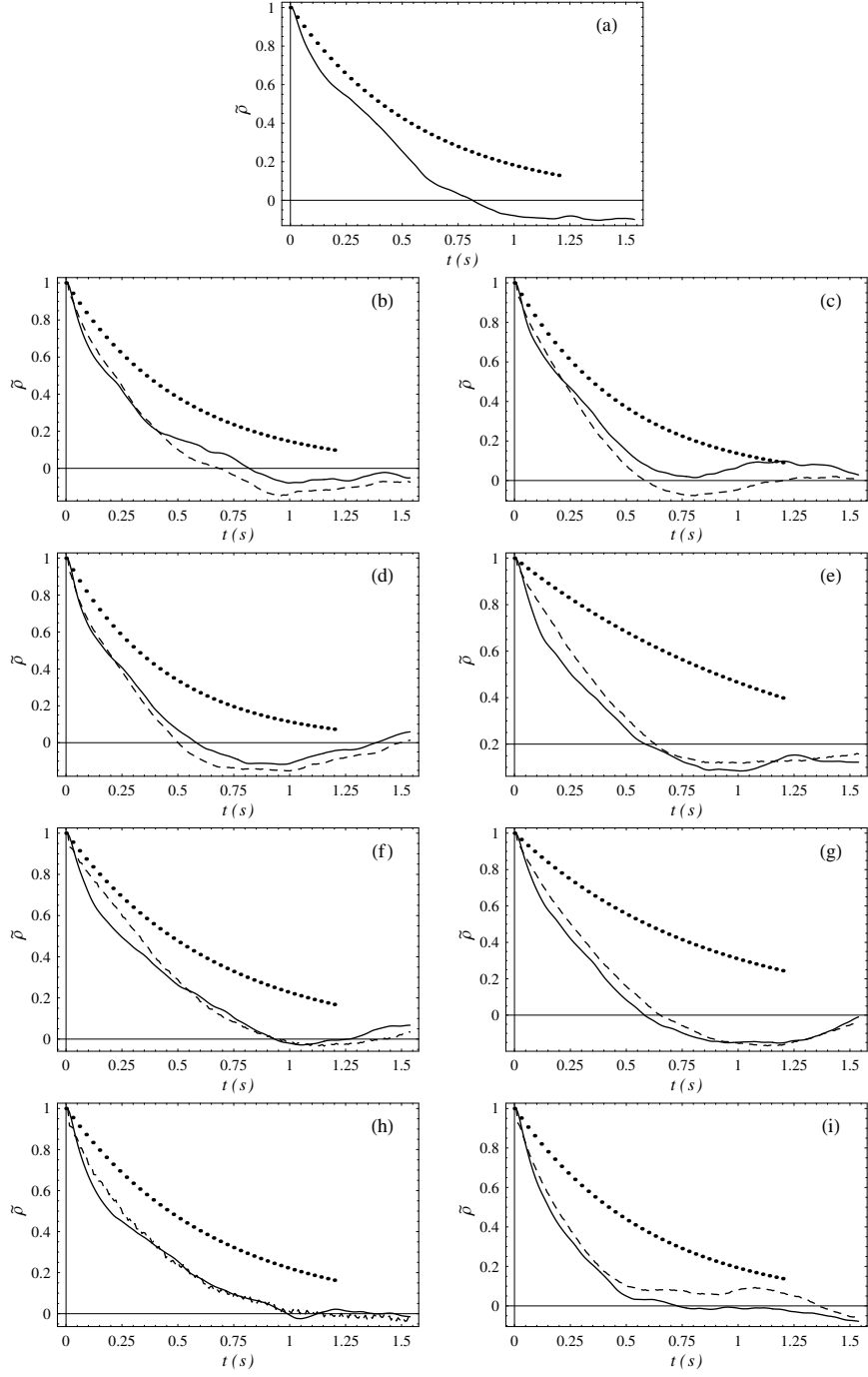


Figure 4: Autocorrelation functions of the number of moving beads (solid line) and the solid discharge (dashed lines). Dotted lines stand for the theoretical autocorrelation function (2.21), when the autocorrelation time \hat{t}_c is evaluated using equation (2.22). Experiments (a-i).

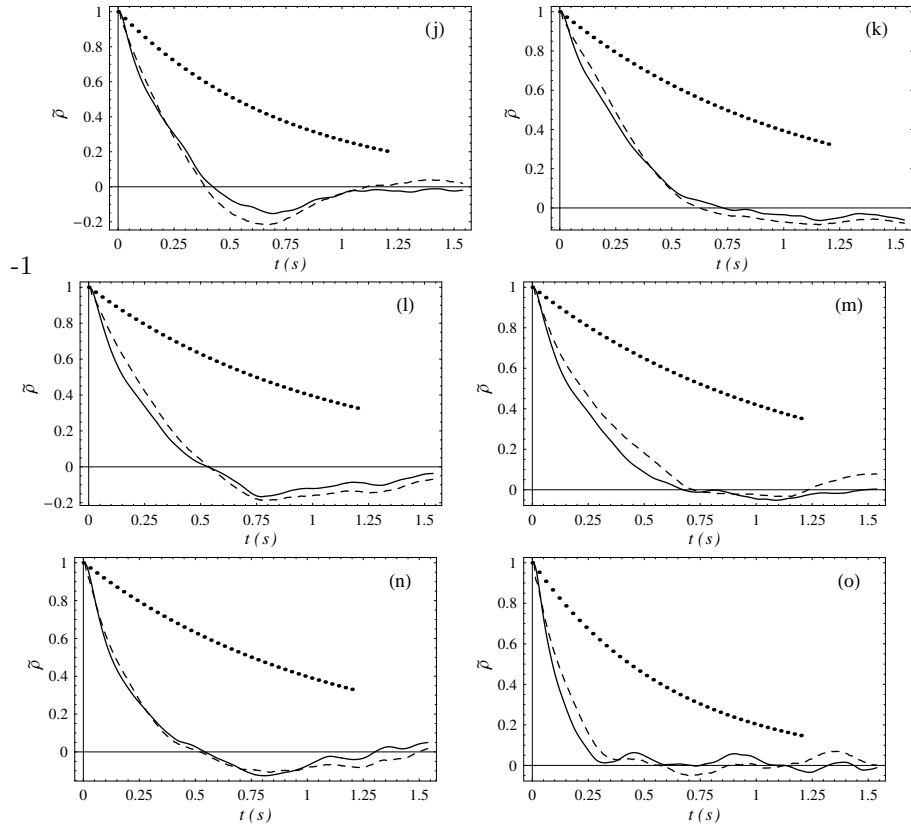


Figure 5: Continuation of figure 4 for experiments (j–o).

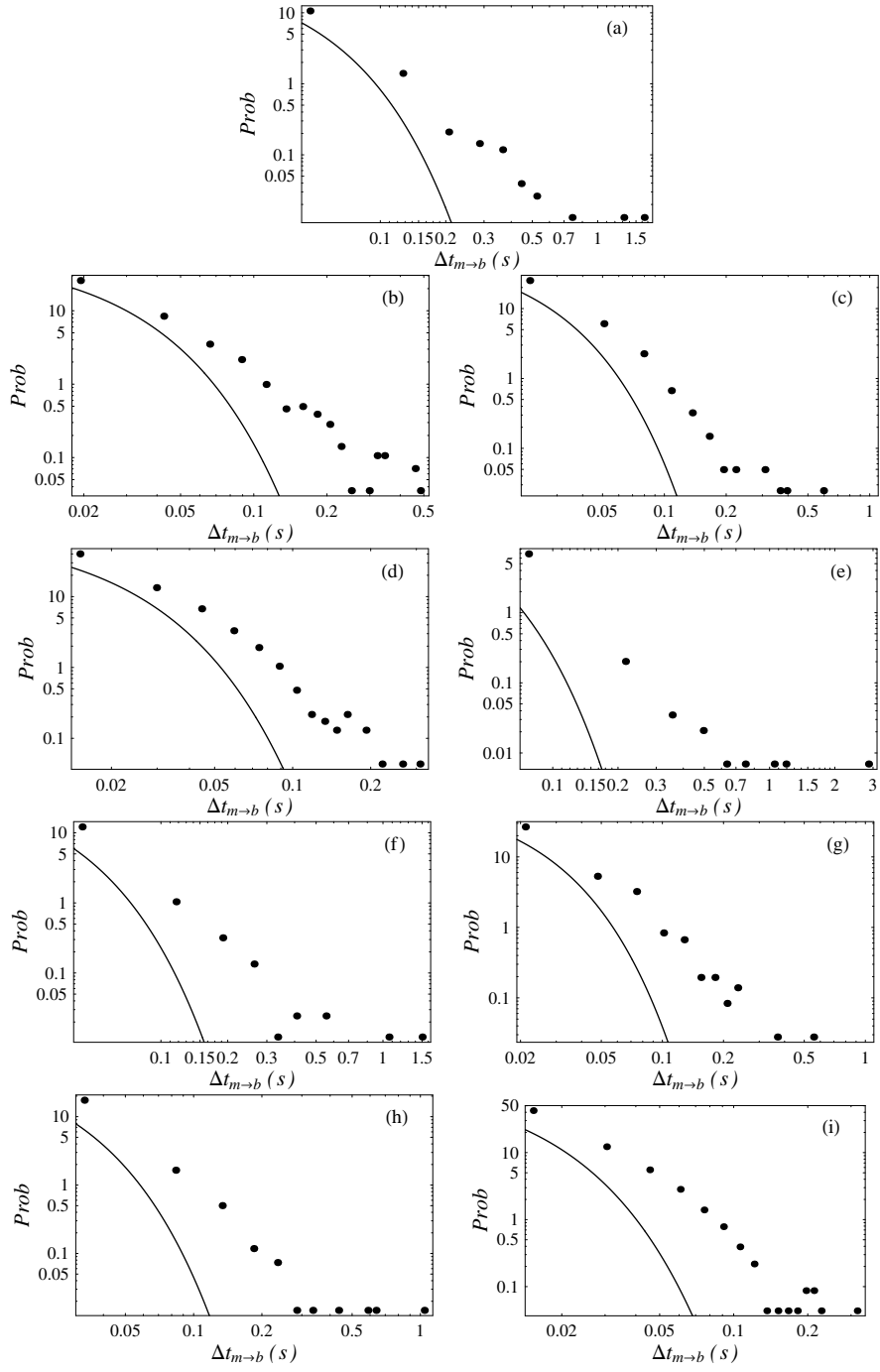


Figure 6: Probability distribution of lag times: dots represent empirical probabilities, while the solid line stands for the theoretical curve (2.27). Experiments (a-i).

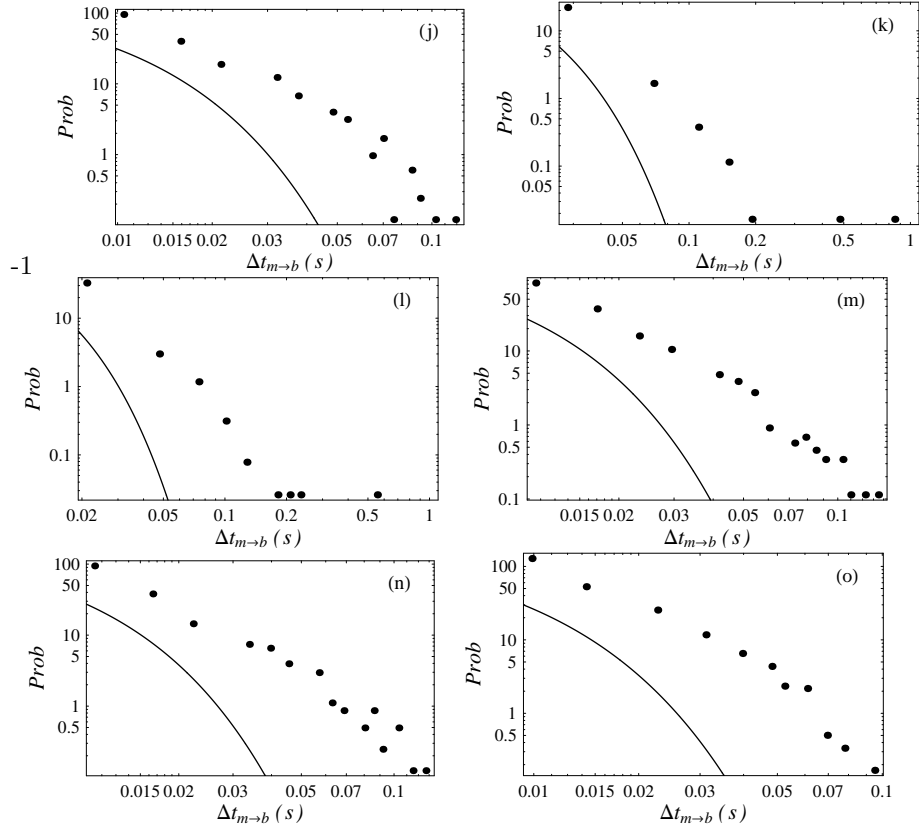


Figure 7: Continuation of figure 6 for experiments (j–o).

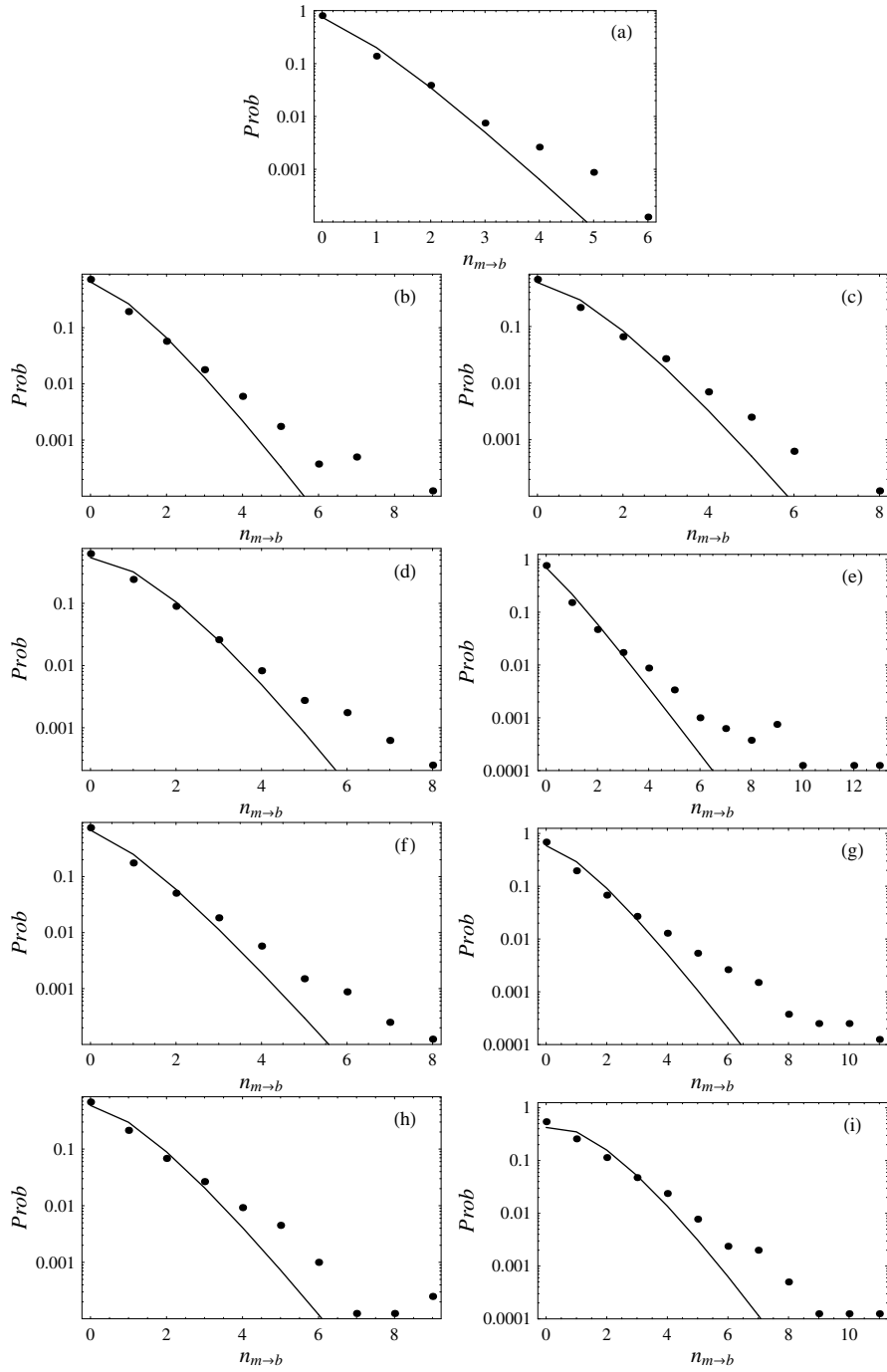


Figure 8: Probability distribution of the number of particles that come to a halt during a time interval δ : dots represent empirical probabilities, while the dashed line represents the theoretical distribution (2.28). Experiments (a-i).

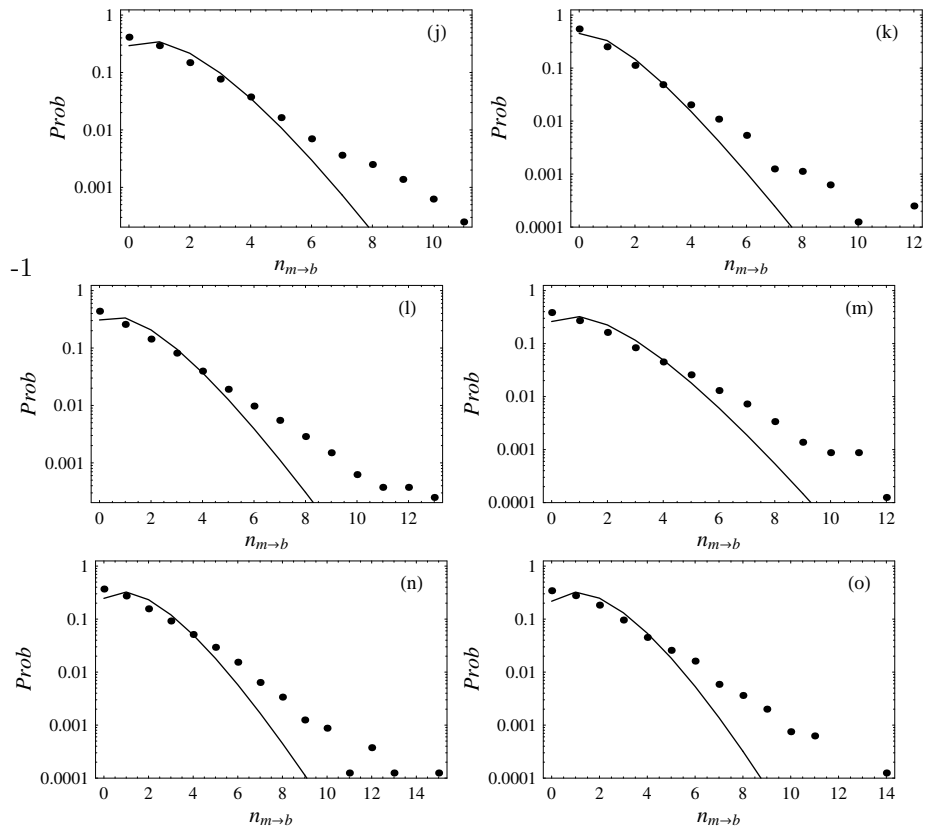


Figure 9: Continuation of figure 8 for experiments (j–o).